Zhang *et al. Cell Communication and Signaling* (2025) 23:195
https://doi.org/10.1186/s12964-025-02179-y

Cell Communication and Signaling

RESEARCH Open Access

Probiotics promote cellular wound healing responses by modulating the PI3K and TGF-β/Smad signaling pathways

Sixuan Zhang[1], Yvonne Elbs-Glatz[1], Siyuan Tao[1], Steven Schmitt[2], Zhihao Li[1*], Markus Rottmar[1*], Katharina Maniura-Weber[1*] and Qun Ren[1*]

Abstract

Background Skin wound healing represents a dynamic and intricate biological process involving the coordinated efforts of various cellular and molecular components to restore tissue integrity and functionality. Among the myriads of cellular events orchestrating wound closure, fibroblast migration and the regulation of fibrosis play pivotal roles in determining the outcome of wound healing. In recent years, probiotic therapy has emerged as a promising strategy for modulating wound healing and fibrosis. Here, we aim to investigate the effect of bacterial probiotics on cell migration and anti-fibrotic response of human dermal fibroblast (HDFs).

Methods Probiotic mixture BioK was co-cultured with HDFs in vitro to assess its impact on fibroblast migration, gene expression, and protein production associated with important processes in wound healing. Gene expression was investigated by transcriptomic analysis and confirmed by RT-qPCR. Protein levels of the identified genes were evaluated by ELISA. The role of lactic acid, produced by BioK, in mediating pH-related effects on fibroblast activity was further examined.

Results We observed that BioK effectively promoted HDFs migration in vitro, which was found to be related to the up-regulation of genes involved in the phosphoinositide 3-kinase (PI3K) signaling pathways such as Paxillin, PI3K, PKC and ITG-β1. Interestingly, we also found that BioK down-regulated the expression of Nox-4, α-SMA and Col-I in TGF-Smad signaling pathways, which are involved in the differentiation of fibroblasts to myofibroblasts, and extracellular matrix type I collagen production, demonstrating its potential in reducing formation of fibrosis and scars. One of the acting factors for such down-regulation was identified to be BioK-produced lactic acid, which is known to lower the surrounding pH and to play a major role in fibroblast activity and wound healing.

*Correspondence:
Zhihao Li
zhihaoli91@gmail.com
Markus Rottmar
markus.rottmar@empa.ch
Katharina Maniura-Weber
katharina.maniura@empa.ch
Qun Ren
qun.ren@empa.ch

Full list of author information is available at the end of the article

Conclusions This study demonstrates BioK's beneficial effects on fibroblast migration and its potential to mitigate fibrosis through pH modulation and pathway-specific gene regulation. These findings enhance our understanding of probiotic action on wound healing and offer promising therapeutic insights for the reduction of scar formation.

Clinical trial number Not applicable.

Graphical Abstract

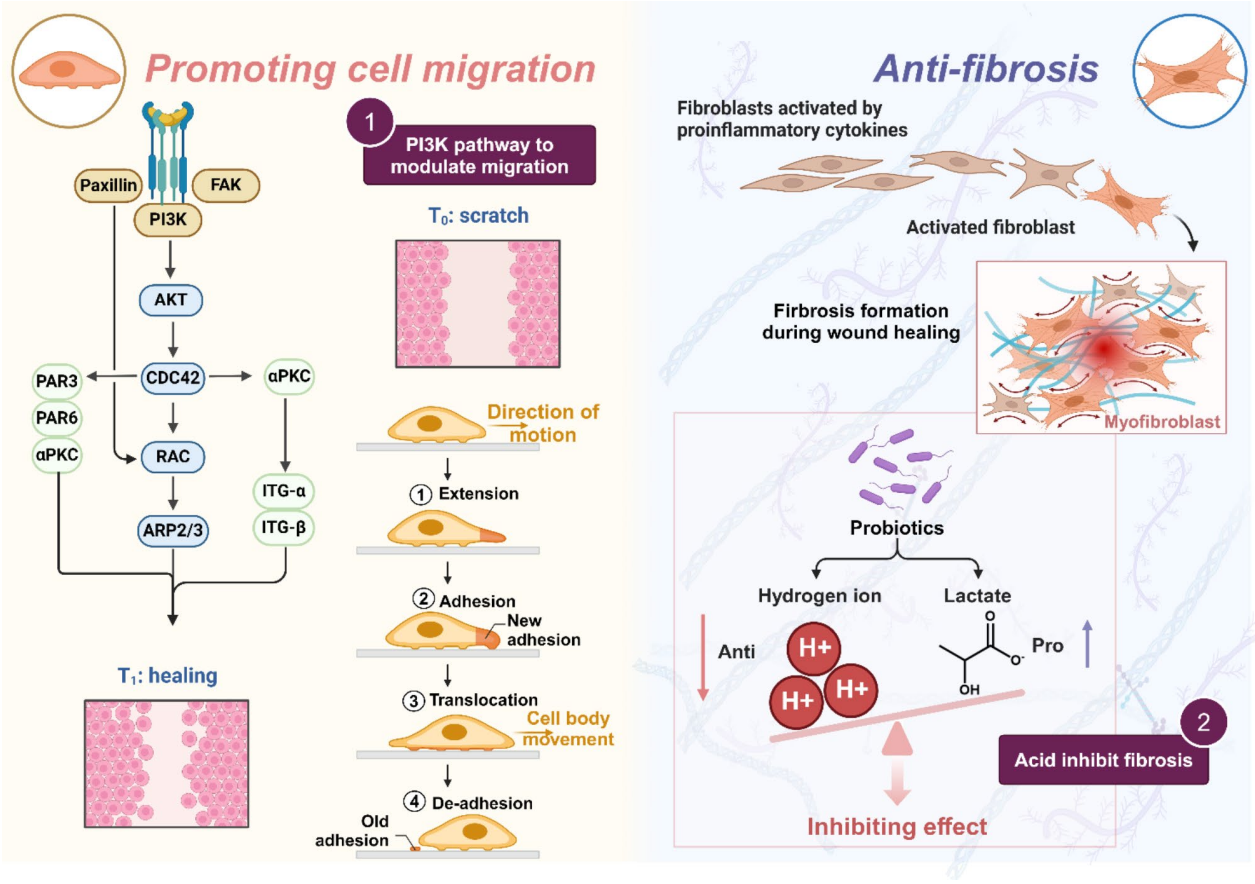

Keywords Probiotics, Wound healing, PI3K pathway, Anti-fibrosis, TGF-β /Smad pathway, Myofibroblast differentiation

Background

Skin wound healing represents a dynamic and intricate biological process involving the coordinated efforts of various cellular and molecular components to restore tissue integrity and functionality [1]. Among the myriad of cellular events orchestrating wound closure, fibroblast migration and the regulation of fibrotic events play pivotal roles in determining the outcome of wound healing [2]. Fibroblasts, the principal effector cells in wound repair, are responsible for synthesizing and remodeling the extracellular matrix (ECM), thereby facilitating tissue regeneration [3]. Efficient fibroblast migration is essential for timely wound closure and tissue regeneration [4–6]. Moreover, the balance between ECM synthesis and degradation is crucial for maintaining tissue homeostasis during wound healing [7]. Excessive deposition of ECM components, known as fibrosis, can lead to impaired tissue function and compromised wound healing outcomes [8, 9]. Cutaneous wound healing represents a significant clinical challenge, with an increasing need for innovative therapeutic strategies to improve outcomes and reduce complications. In recent years, probiotic therapy has emerged as a promising strategy for modulating wound healing and fibrosis [8, 10, 11].

One mechanism through which probiotics may act on fibroblasts to treat skin-related diseases is by modulating the phosphatidylinositol 3-kinase (PI3K)/Akt signaling pathway, a critical regulator of cell motility and cytoskeletal dynamics [12]. For instance, one study highlights that the use of multiple probiotic strains can potentially alert the gut mucosal immune system and promote wound healing [13]. Another recent in vivo study has shown

that *Lactobacillus reuteri* extracts accelerate oral mucosal wound healing by enhancing the function of gingival mesenchymal stem cells through upregulation of the expression of activated-β-catenin and transforming growth factor β1 (TGF-β1) and by enhancing the PI3K/Akt pathway [14].

Similarly, in recent years, probiotic therapy also has garnered increasing attention for its multifaceted effects on host physiology, including modulation of the immune response, attenuation of inflammation, and maintenance of tissue homeostasis [15–17]. Dou et al. found that *L. casei*-loaded silk fibroin/sodium alginate scaffolds induced M2 polarization of macrophages, increased angiogenesis, regulated collagen ratios, and alleviated the endoplasmic reticulum stress, thereby promoting scarless wound healing in vivo [18]. Satish et al. reported that application of *L. plantarum* significantly reduced both type I collagen mRNA concentrations and total collagen protein accumulation in infected wounds, consistent with reduced scarring [19].

Despite the accumulating evidence supporting the therapeutic potential of probiotics to promote wound healing and reduce fibrosis, several knowledge gaps and challenges remain. Especially, the molecular mechanisms underlying probiotic-fibroblast interactions is ill-defined. Additionally, understanding which active components of probiotics inhibit fibrosis formation is of great significance for optimizing probiotic therapy and achieving clinical translation. Here, we used the probiotic mixture BioK to investigate its impact on fibroblast migration and fibrosis. Our results show that the probiotic mixture promotes the migration rate of fibroblasts, which was found to be related to an upregulation of the PI3K signaling pathway. In addition, we also revealed that probiotics regulate environmental pH through lactic acid secretion, which affects the differentiation process of fibroblasts to myofibroblasts, thus potentially inhibiting the fibrotic process and scar formation. Our study provides insights into the underlying mechanisms behind the probiotic's promotion of cell migration and inhibition of differentiation, which could contribute to enhanced treatment of skin wounds and scar prevention therapies.

Materials and methods

Bacteria culture

BioK® capsules containing *L. acidophilus CL1285*®, *L. casei LBC80R*® and *L. rhamnosus CLR2*® were purchased (Laval, Canada) and grown at 37 °C in MRS medium (DeMan, Rogosa and Sharpe), which contains dipotassium hydrogen phosphate (2 g/L), glucose (20 g/L), Tween (1 mL/L), tri-ammonium citrate (2 g/L), sodium acetate (5 g/L), magnesium sulfate heptahydrate (0.2 g/L), meat extract (10 g/L), casein peptone (10 g/L), yeast extract (5 g/L) and manganous sulfate (0.05 g/L). The bacterial strains were stored in 25% glycerol, 25% water, and 50% broth at -80 °C. To monitor bacterial growth, the optical density (OD) of the bacterial culture was measured at 600 nm using a Biophotometer Plus (Eppendorf). All chemicals and reagents were purchased with analytical purity from Sigma-Aldrich (Buchs, Switzerland) and applied as received unless noted otherwise.

Culture of human dermal fibroblast cells (HDFs)

HDFs (PromoCell) were cultured in T-75 flasks with 15 mL Dulbecco's Modified Eagle Medium (DMEM) containing 10% fetal calf serum (FCS) and 1% glutamine in a 37 ℃ incubator with 5% (v/v) CO_2. DMEM with 10% FCS and 1% glutamine was used as proliferation medium, Roswell Park Memorial Institute (RPMI 1640) with 1% horse serum (HS) and 1% glutamine as starvation medium and RPMI with 1% HS, 1% glutamine and 2 ng/ml transforming growth factor beta-1 (TGF-β) as differentiation medium in differentiation experiments.

Growth curves of BioK at different concentrations

BioK, at the end of the preculture period, was diluted in starvation medium, at multiplicity of infection (MOI) ratios 0.01, 0.1, 1 and 10. 200 µL of each conditioned medium were transferred to a 96-well plate with three replicates per group. The kinetics of growth curves were recorded by a micro-plate reader (Synergy™ H1) for 24 h, with continuous linear shaking at 37 ℃ and optical density (OD) being read at 600 nm every 30 min.

Cytocompatibility of BioK to HDFs

HDFs were seeded at a density of 5,000 cells per well in a 96-well plate with proliferation medium and incubated overnight to allow for cell attachment. After that, 200 µl of starvation medium containing BioK at MOI of 0.01, 0.1, or 1 were added for cytocompatibility assays. Cells treated with 0.1% Triton X-100 were used as negative control. The cells were incubated at 37 ℃ and 5% CO_2 for 24, 48 and 72 h respectively; the medium was changed every day. Cell viability was determined using PrestoBlue Kit according to the manufacturer's instructions using a Mithras plate reader, with fluorescence excitation wavelength at 547 nm and emission wavelength at 582 nm.

HDFs cell migration assays

HDFs were seeded in a culture-insert petri dish (ibidi culture-insert 2 well, ibidi GmbH, Martinsried, Germany) at a density of 5×10^4 cells per well. After allowing the cells to attach overnight, the culture insert was removed, and the dishes were washed with pure DMEM to remove non-adherent cells. Fresh proliferation medium containing different concentrations of BioK probiotics was added and the cells were imaged every 3 h in the first 12 h and at time point 24 h using a light microscope (x25

magnification, Olympus, Japan). Cell areas were determined using Image J analysis. For each image, the area between one side of the gap and the other was measured. Quantification of gap closure was performed by comparing the area of the gap at the set time points according to the equation:

$$\text{Percentage of gap closure} = \frac{[\text{S}(\text{t} = 0\text{h}) - \text{S}(\text{t} = \text{x})]}{[\text{S}(\text{t} = 0\text{h})]} \times 100$$

Where t = x is a specific time point after removal of the insert, and S means the surface area of the gap. The experiment was performed three times with triplicate samples within each experiment.

RNA-Seq library construction and data analysis

Total RNA was extracted at the end of the cell migration assay according to the above method. The library was checked with Qubit and real-time PCR for quantification and bioanalyzer (Novogene Co.,Ltd., UK) for size distribution detection. Quantified libraries were pooled and sequenced on Illumina platforms, according to effective library concentration and data amount. For data analysis, raw data (raw reads) of fastq format were first processed through fastp software. In this step, clean data (clean reads) were obtained by removing reads containing adapter, reads containing ploy-N and low-quality reads from raw data. All the downstream analyses were based on clean data with high quality. Reference genome and gene model annotation files were downloaded from the genome website directly. The index of the reference genome was built using Hisat2 v2.0.5 and paired-end clean reads were aligned to the reference genome using Hisat2 v2.0.5. Differential expression analysis of two conditions/groups (two biological replicates per condition) was performed using the DESeq2 R package (1.20.0). DESeq2 provides statistical routines for determining differential expression in digital gene expression data using a model based on the negative binomial distribution [20, 21]. The resulting P-values were adjusted using the Benjamini and Hochberg's approach for controlling the false discovery rate. Genes with an adjusted P-value ≤ 0.05 found by DESeq2 were assigned as differentially expressed.

Gene Ontology (GO) enrichment analysis of differentially expressed genes was implemented by the clusterProfiler R package, in which gene length bias was corrected [22]. GO terms with Padj less than 0.05 were considered significantly enriched by differentially expressed genes. KEGG is a database resource for understanding high-level functions and utilities of the biological system, such as the cell, the organism and the ecosystem, from molecular-level information, especially large-scale molecular datasets generated by genome sequencing and other high-throughput experimental technologies (http://www.genome.jp/kegg/) [23]. We used the clusterProfiler R (v 3.8.1) package to test the statistical enrichment of differential expression genes in KEGG pathways.

Inhibition of PI3K pathway

PI3K inhibitor 2-(4-Morpholinyl)-8-phenyl-1(4 H)-benzopyran-4-one hydrochloride (LY294002, Merck, Switzerland) was dissolved in DMSO to obtain a stock solution by following the product instructions. Based on the preliminary experiments (**Supporting information 1**), signaling pathway validation experiments were performed using differentiation media containing 1 μM LY294002.

Differentiation of HDFs to myofibroblasts and anti-fibrosis study

In the differentiation experiments, the experimental conditions were divided into four groups based on the additives: (i) starvation medium (blank Ctrl), (ii) differentiation medium (TGF-β, positive control), (iii) starvation medium with BioK probiotics at a MOI ratio of 1 (BioK), and (iv) differentiation medium with BioK probiotics at MOI 1 (BioK + TGF-β).

For immunofluorescence staining analysis, cells were cultured in proliferation medium in 96-well plates at a density of 20,000 cells per well. For relative gene expression analysis, cells were cultured in proliferation medium in 48-well plates at a density of 30,000 cells per well. Following an overnight incubation to allow for cell attachment, the medium was replaced with the appropriate medium as per the experimental design. The co-culture period lasted for 72 h, with the medium being refreshed every 24 h.

Differentiation medium with reduced buffer strength

For medium with reduced buffer capacity, 10.4 g buffer-free RPMI 1640 medium powder were dissolved in 100 mL sterile H_2O to obtain 10x stock medium solution. During this process, the pH of the solution was adjusted to 4.0 with 1 M HCl to facilitate the dissolution of the powder. The stock solution was filtered (membrane with a pore size of 0.4 μm) and diluted to 1x working concentration with sterile water. Addition of different volumes of 7.5% sodium bicarbonate solution resulted in media with different buffer strength, where the gradient difference was 10%. Complete medium buffered with 26.7 mL of 7.5% sodium bicarbonate solution per liter served as control (100% buffered medium). Media were supplemented to a final concentration with 1% horse serum (HS) and 2 ng/mL of TGF-β factor before performing differentiation experiments. Medium containing 40% buffer

(10.68 mL of 7.5% sodium bicarbonate solution per liter) was chosen as a reference to study the effect of acid on differentiation behavior.

Qualitative observation of myofibroblast differentiation by immunofluorescent staining

After 72 h of culture, HDFs were stained for representative makers of fibrosis (i.e. alpha-smooth muscle actin (α-SMA) and alpha1 type I collagen (Col-I)). Cells were fixed with 4% paraformaldehyde for 10 min, washed three times with PBS, and exposed to 0.1% TritonX-100 for 10 min to increase cell membrane permeability. The cells were then blocked with 1% BSA (in PBS) for 30 min and incubated in BSA (in PBS) containing anti-Col-I antibody with dilution 1:1000 at 4 ℃ overnight. The primary antibody was then removed and cells were rinsed with PBS. Secondary antibody fluorescein isothiocyanate (FITC)-labeled goat anti-rabbit IgG, was diluted 1:400 in 1% BSA and cells were treated for 2 h at room temperature (RT) in the dark. After thorough rinsing, the cytoskeleton was stained with Alexa Fluor 488-labelled phalloidin at a dilution of 1:200 while the nuclei were stained with 4',6-diamidino-2-phenylindole (DAPI) at a dilution of 1:1000. Samples were imaged using a Zeiss LSM780 confocal laser scanning microscope. When staining for α-SMA, Alexa Fluor 488 conjugated α-SMA antibody at 1:800 dilution and Alexa Fluor 546- labelled phalloidin at a 1:200 dilution were used. Detailed information about antibodies and chemicals for immunofluorescent staining is shown in Table 1 below.

Quantitative analysis Col-I

HDFs were seeded in starvation medium at a concentration of 50,000 cells/well in 12-well plates. After overnight culture, medium was exchanged using treatment conditions as stated in the myofibroblast differentiation and anti-fibrosis section. The collagen concentration of the cell matrix after differentiation was measured using a Sircol Soluble Collagen Assay Kit (Tebubio, Germany) according to the manufacturer's instructions.

Table 1 Information about antibodies and chemicals

Antibodies	Catalog number	Supplier
FITC-conjugated antibody α-SMA	F3777	Sigma
Primary antibody Col-I	C2456	Sigma
Secondary antibody Alexa Fluor546 goat-anti-mouse IgG	A11030	Invitrogen
Alexa Fluor 488 phalloidin	A12379	Invitrogen
Alexa Fluor 546 phalloidin	A22283	Invitrogen
DAPI	D9542	Sigma

pH measurement

The pH value of medium was measured at 0 and 24 h using a 913 pH meter (Metrohm, Switzerland). In the differentiation experiment with reduced buffer capacity, the medium in each group was collected and filtered with 0.45 µm filter (Macherey-Nagel, Germany) to remove bacteria for the pH measurement at 37 ℃ in a water bath after 0, 24, 48 and 72 h of culture.

HPLC measurement

High Performance Liquid Chromatography (HPLC) analysis was carried out on samples containing lactate. The solution was passed through an ACQUITY UPLC (H-Class, Waters, USA) equipped with a photo diode array detector (PDA). Measurements were performed with an Aminex HPX-87 H column (BioRad, USA). The measurement conditions were chosen as follows: column temperature of 60 °C, flow of 0.4 mL/min of 5 mM H_2SO_4 as the eluent (isocratic) and injection volume of 5 µL.

Gene expression analysis by reverse transcriptase quantitative polymerase chain reaction (RT-qPCR)

At the end of culture periods, the relative gene expression levels for various markers were measured. Total RNA was extracted from cells using a Total RNA Kit following the manufacturer's instructions. Cells were collected and lysed with TRIzol buffer (ThermoFisher). Total RNA was extracted using an RNA Mini Kit (Invitrogen) following the manufacturer's instructions. The extracted RNA was reverse transcribed into cDNA using iScript cDNA Synthesis Kit (BIO-RAD). Quantitative real-time PCR (RT-PCR) reactions were performed on a CFX Opus 384 Real-time PCR system and monitored using SYBR Green Supermix (BIO-RAD). For the analysis of target genes and the reference gene GAPDH, RT-PCR was performed at 95 ℃ for 3 min followed by 40 cycles of denaturation for 10 s at 95 ℃, 30 s annealing and elongation at 60 ℃. The level of expression of each target gene was then calculated as $2^{-\Delta\Delta CT}$. All primers shown in Table 2 below were purchased from Microsynth AG (Balgach, Switzerland).

Statistical analysis

All experiments were performed independently at least twice and quantified with at least three parallel samples per condition in each experiment. The exact numbers of experimental and technical replicates are provided in the figure captions. The results are expressed as the mean ± standard deviation of each sample. One-way ANOVA (analysis of variance) with a Tukey's post-hoc test was used to assess statistically significant differences between groups under identical treatments. A difference with a p-value of <0.05 was considered statistically significant.

Table 2 Primers for RT-PCR

Gene	Forward Primer (5′-3′)	Reverse Primer (5′-3′)
GAPDH	CTACTGGCGCTGCCAAGGCTGT	GCCATGAGGTCCAC-CACCCTGT
α-SMA	TGAGAAGAGTTACGAGTTGCC	GATGCCAGCAGACTCCATCC
Nox4	ATCTGGCTCTCCATGAATGTCCTG	ACACAATCCTAGCCCCAA-CATCTG
Col-I	CAGCCGCTTCACCTACAGC	TTTTGTATTCAATCACT-GTCTTGCC
Smad2	ACCGAAATGCCACGGTAGAA	TGGGGCTCTGCACAAAGAT
Smad3	CATCGAGCCCCACAATA	GTGGTTCATCTGGTGGT-CACT
Paxillin	CTGATGGCTTCGCTGTCGGATT	GCTTGTTCAGGTCAGACT-GCAG
PI3K	GGTAATCGGAGGATAGGGCAGT	CGGCAGTAT-GCTTCAAGGATGAC
ITG-β1	GGCCTTGCATTACTGCTGAT	CAGTGTTGTGGGATTTGCAC
PKC	GCCTATGGCGTCCTGTTGTATG	GAAACAGCCTCCTTGGA-CAAGG

Results and discussion

Establishing a co-culture model of probiotics and human dermal fibroblasts (HDFs)

To study the effect of wound healing using probiotic bacteria under laboratory conditions, we first established an in vitro assay that enables co-culture of HDFs and BioK. To this end, we evaluated the appropriate probiotic dosage in order to prevent premature death of HDFs by bacterial overgrowth. BioK and HDFs were incubated with four different infection ratios, namely, multiplicity of infection (MOI) of 0.01, 0.1, 1 and 10 for BioK and HDFs, respectively. It was observed that MOI 10 led to a dramatic growth of BioK (Fig. 1A), and the co-culture medium became turbid after 24 h of incubation. Since excessive probiotic growth in the co-culture system leads to depletion of nutrients and accumulation of metabolic wastes in the medium, which can ultimately interfere with the physiological activity of HDF cells, MOI 10 was not included in the further study. MOI 0.01, 0.1 and 1 did not show any obvious growth compared with the control (pure medium) under the same growth condition (Fig. 1A). When co-cultured with HDFs these concentrations also had no negative impact on HDF viability (Fig. 1B).

Probiotic BioK promotes cell migration

After confirming the cytocompatibility of probiotics BioK, we systematically studied the effect of BioK on HDF migration using a cell migration assay. After 24 h of culture, all groups with BioK showed enhanced cell migration with 45.1%, 21% and 14.1% of gap closure using MOI 1, 0.1 and 0.01, respectively, much higher compared to the control group without BioK at 6.5% (Fig. 1C, D). After 48 h, the closure of the gap area with the MOI 1 group reached 97.0%, the highest among all tested groups, while the control group was only 50.5% (Fig. 1E). We further compared the cell migration of MOI 1 and blank control groups by analyzing vinculin, a typical protein associated with focal adhesions and cell movement. Confocal laser scanning microscopy (CLSM) images showed qualitatively higher abundance of vinculin in cells treated with probiotics at MOI 1 when compared to the blank control (Fig. 1F). In agreement with the here described positive effect of probiotics on cell migration, similar observations have been reported previously about the promoting effect of mixed probiotics on migration of colonic subepithelial myofibroblasts [13], where stimulation with 10^4 CFU/mL of a probiotic mix promoted migration by 133.8%, which was however not observed at a lower concentration of 10^2 CFU/mL. We further observed a positive correlation between bacterial cell number (in the range of 10^3-10^5 CFU/mL) and HDF migration.

Transcriptome analysis reveals BioK modulated the PI3K pathway

To further study the potential mechanism underlying the promoting effect of BioK on cell migration, we conducted RNA-seq analysis of the BioK treated HDFs using a previously described method [24]. We performed principal component analysis (PCA) on the gene expression value (FPKM) of all samples to evaluate intergroup differences and intragroup sample variation. Overall, parallel samples from the same experimental group are clustered and samples from different experimental groups separated. The greatest differences of transcriptomic profiles were observed between the control and MOI 1 groups (Fig. 2A). Further, we used mainstream hierarchical clustering for the FPKM values of genes and homogenized the row (Z-score). The genes or samples with similar expression patterns in the heat map are gathered. The color in each grid does not reflect the gene expression value, but the value obtained after homogenizing the expression data rows (generally between – 2 and 2). Comparison of the global gene expression patterns between untreated groups and those treated with different infection ratios indeed revealed the most distinct features in MOI 1 and control (Fig. 2B). Compared to the control, 1394 genes were upregulated and 1749 genes downregulated in MOI 1 culture conditions (Fig. 2C). To clarify the molecular functions and biological processes involved behind these genes and the associated signaling pathways, we performed Gene Ontology (GO) and Kyoto Encyclopedia of Genes and Genomes (KEGG) pathway enrichment analysis. The GO enrichment analysis indicates the cell adhesion molecule binding genes represent the most relevant molecular function (Fig. 2D), whereas the KEGG enrichment shows the most significant

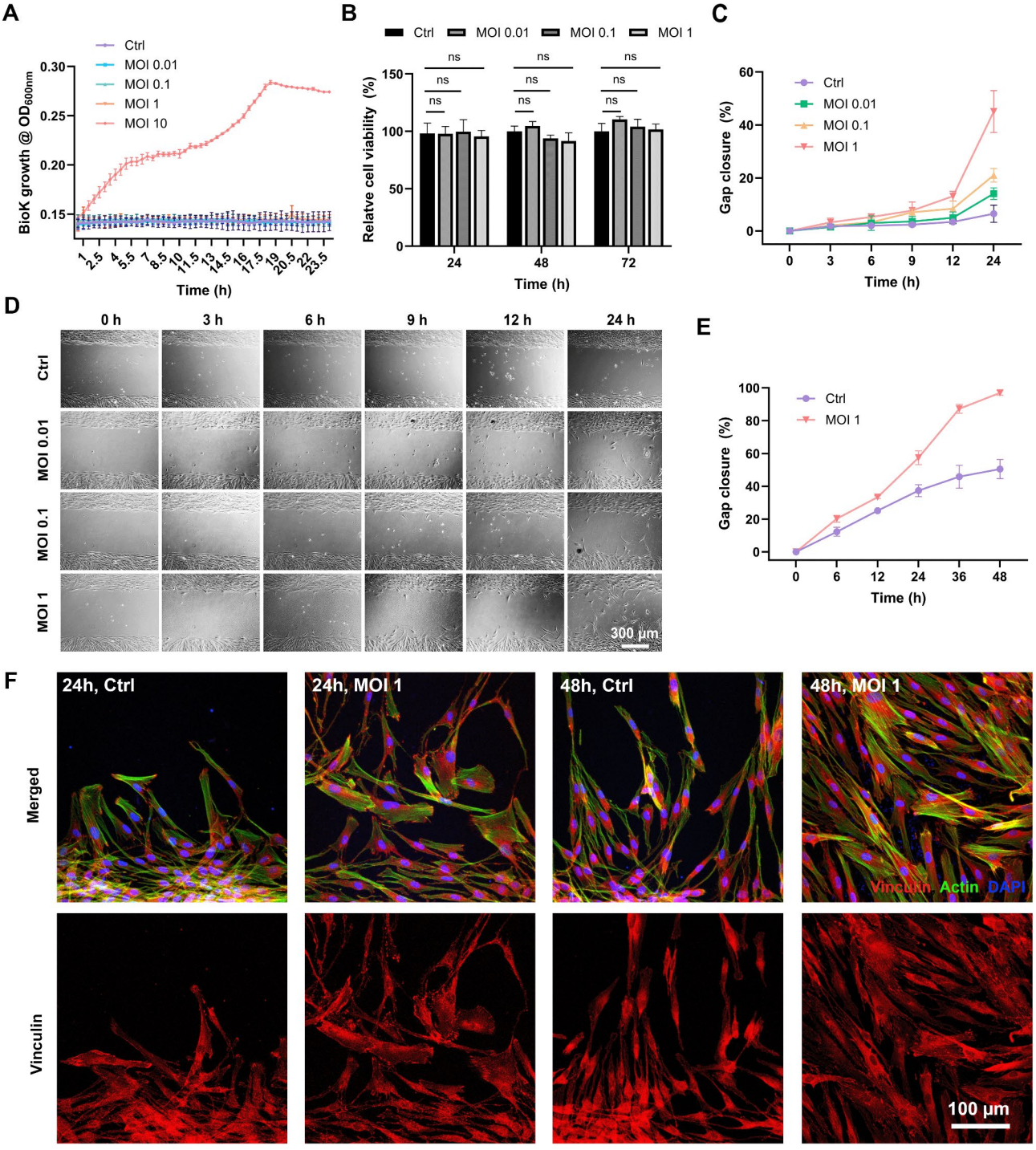

Fig. 1 Promoting effects of probiotics on HDF migration. (**A**) Growth curves of BioK (MOI 0.01 to 10) in HDF culture medium with different infection ratios; (**B**) Effect of different infection ratios of BioK (MOI 0.01 to 1) on the viability of HDFs; (**C**) Quantitative analysis of in vitro gap closure in the presence of BioK (MOI 0.01 to 1) up to 24 h (n = 3) by employing ImageJ; (**D**) Light microscopy images illustrating the migration of HDF during 24 h co-culture with BioK.; (**E**) Quantitative analysis of gap closure in the presence of BioK/ MOI 1 during 48 h (n = 3) by ImageJ; (**F**) Immunofluorescence staining for F-actin (green), vinculin (red) and nuclei (blue), F-actin and vinculin being relevant for cell migration of fibroblasts after co-culture with Bio K for 24 hand 48 h. 'Ctrl' refers to control group without BioK. Error bars represent the standard deviation. $n = 3$, *: $P < 0.05$ and *ns*: not significant ($P > 0.05$) by ANOVA with a Tukey's post-hoc test

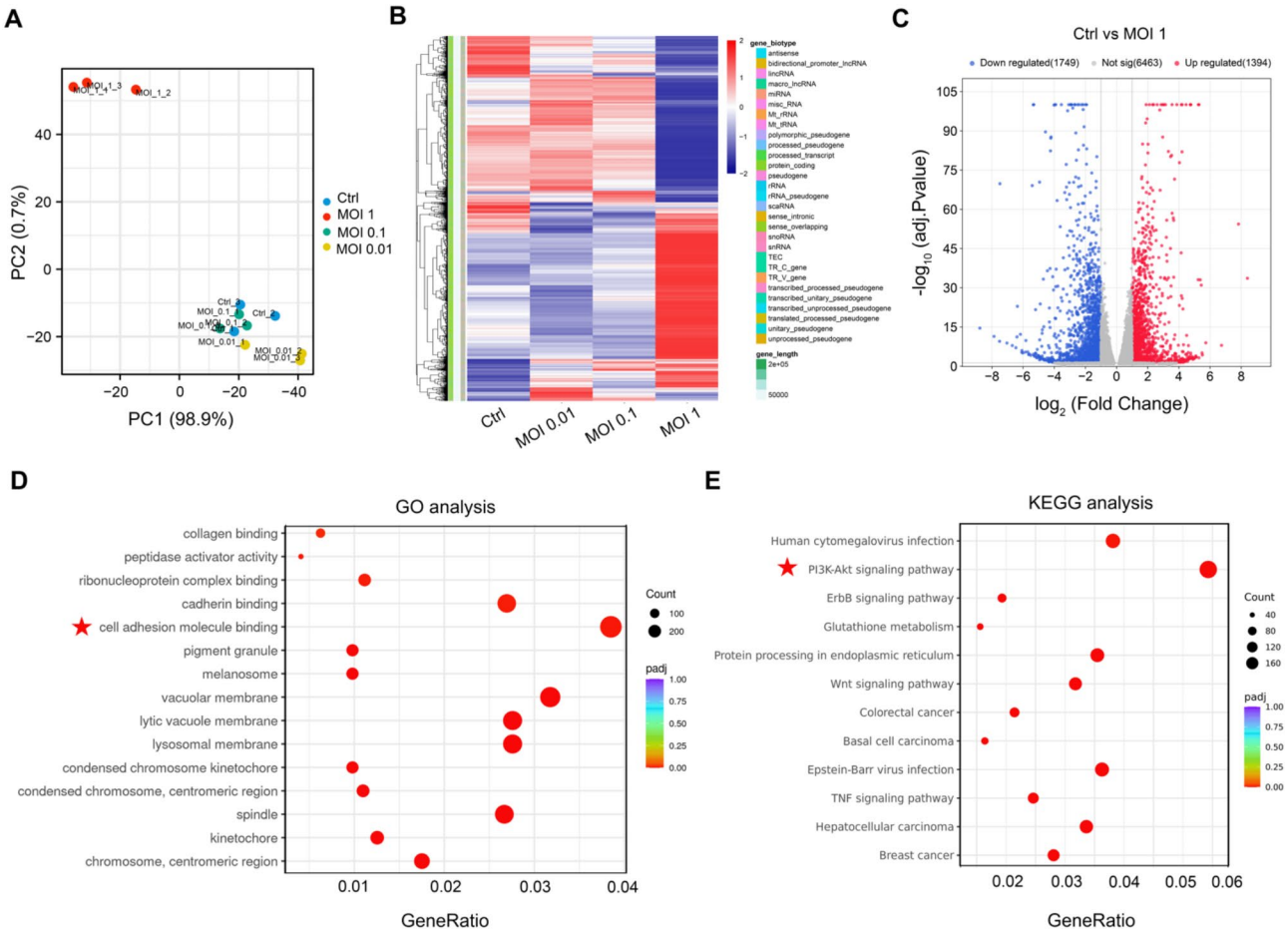

Fig. 2 Transcriptome assessment of HDFs after treatment with BioK by using RNA-seq. (**A**) Principal component analysis. The samples between groups are dispersed and the samples within groups are gathered together. (**B**) Differential expression gene clustering heatmap. Colors indicate genes with high (red) and low (blue) expression levels (fold change ≥ 2 and $P \leq 0.05$). (**C**) Differential Gene Volcano Map. Red dots: significantly upregulated genes; blue dots: downregulated genes; gray dots: genes that are not significantly changed. (Padj < 0.05, ≥ 2-fold expression levels). (**D**) GO Enrichment Analysis Scatter Plot. The abscissa is the ratio of the number of differential genes linked with the GO Term to the total number of differential genes, and the ordinate is GO Term. (**E**) KEGG enrichment scatter plot. The abscissa in the graph is the ratio of the number of upregulate differential genes on the KEGG pathway to the total number of differential genes, and the ordinate is KEGG pathway. padj: Adjusted p-value. Generally, GO Terms and KEGG pathways with padj < 0.05 are regarded as significantly enriched. The size of a point represents the number of genes annotated to a specific GO Term/KEGG pathway, and the color from red to purple represents the significant level of the enrichment

upregulation in the MOI 1 treated group for the PI3K-Akt signaling pathway (Fig. 2E).

Probiotics upregulate PI3K-related genes promoting cell migration

To further confirm the KEGG enrichment result and figure out which genes are upregulated in the PI3K signaling pathway in response to probiotics treatment, qPCR was used. Different concentrations of PI3K inhibitor LY294002 were first evaluated for their cytocompatibility with HDFs and BioK probiotics (Fig. S1). The concentration of 1 μM PI3K inhibitor was chosen for further studies due to its clear inhibiting effect on expression of genes involved in the PI3K pathway (Fig. S2).

Upon treatment of fibroblasts with BioK, the relative expression of paxillin, PI3K, PKC and ITG-β1 genes was increased to 1.77-fold, 1.26-fold, 1.48-fold and 1.02-fold of the blank group, respectively (Fig. 3B). These findings are correlated with the results from the RNA-seq analysis. Upon addition of PI3K inhibitor, the relative expression of paxillin, PI3K, PKC and ITG-β1 genes was reduced to 0.67-fold, 0.85-fold, 0.75-fold, 0.68-fold of the blank group, respectively (Fig. 3B). Application of both, BioK and PI3K inhibitor LY294002, rescued their expression to levels comparable or even higher than the untreated control, namely 0.91, 1.14, 0.96, and 0.94-fold of the blank (Fig. 3B). These results demonstrate that all these genes related to the PI3K signaling pathway are involved in modulating the migratory activity of cells upon the application of probiotics.

In our study, BioK acted on different components of the PI3K signaling pathway influencing cell protrusion,

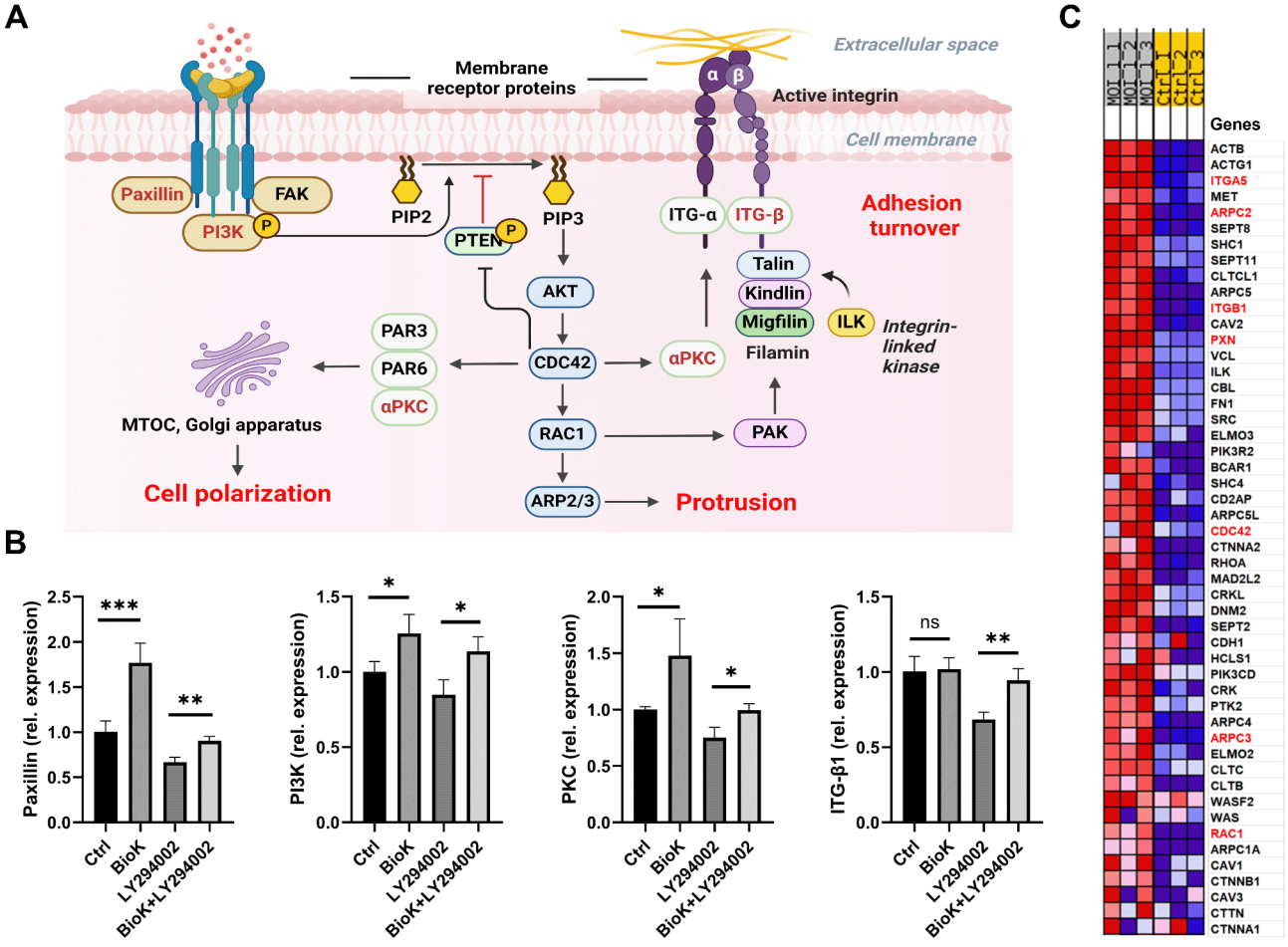

Fig. 3 Upregulation of PI3K-related genes by BioK. (**A**) Schematic of PI3K signaling pathway related to cell migration. Enhancement of cell migration in the presence of probiotics by influencing cell polarization, protrusion and adhesion through PI3K signaling cascades and pathway networks. (**B**) Relative gene expression of paxillin, PI3K, PKC and ITG-β1 in the presence/absence of PI3K inhibitors. 'Ctrl' is the group with neither inhibitor nor BioK. (**C**) GSEA (Gene set enrichment analysis) of KEGG pathway. The genes marked in red are discussed in the Results and Discussion section. 'Ctrl' refers to control group without PI3K inhibitor or BioK. Error bars represent the standard deviation. $n = 3$, *: $P < 0.05$, **: $P < 0.01$, ***: $P < 0.001$, *ns*: not significant ($P > 0.05$) by ANOVA with a Tukey's post-hoc test

polarization and adhesion and with this promoting cell migration as reported in the literature [25–27]. Paxillin is a multidomain adaptor protein that recruits structural and signaling molecules to focal adhesions, the sites of integrin engagement with the extracellular matrix. It plays a crucial role in transducing adhesion and growth factor signals, thereby influencing cell migration and gene expression [28] (overview in Fig. 3A). In a series of experiments on cell migration of P19 cells, primary human renal microvascular endothelial cells and Chinese hamster ovary (CHO)-EphB1 cells, it was shown that phosphorylation of paxillin was required for cell migration, and that phosphorylated paxillin could indirectly activate the essential control gene Rac1 for efficient leading edge protrusion during cell migration [29–31]. Cellular protrusion is also regulated by cell division control protein 42 gene (Cdc42) as it activates the Arp2/3 complex that controls actin polymerization in the same way that the action of the Rac1 gene does [6]. Our results reveal that probiotics can promote the gene expression of paxillin (Fig. 3B) and Rac1 (Fig. 3C). The up-regulation of genes involved in the synthesis of actin, including Cdc42, Arp2 and Arp3 genes, can also be detected in the heat map of Fig. 3C, indicating that probiotics regulate these genes in the PI3K signaling pathway promoting protrusion via modulating the paxillin-Rac-Arp2/3 axis.

Furthermore, Cdc42 is a master regulator of cell polarity in eukaryotic organisms ranging from yeast to humans and is active toward the front of migrating cells [32], and is affected by activation of PI3K/Akt [33–35]. Cdc42 can also affect polarity by localizing the microtubule-organizing center (MTOC) and Golgi apparatus in front of the nucleus, oriented toward the leading edge [36, 37]. The effects of Cdc42 on MTOC position appear to be exerted mainly through a pathway involving the Cdc42 effector PAR6, which exists in a complex

with PAR3 and an atypical protein kinase C (PKC) [38]. In this work, we found that the expression of PI3K and PKC (Fig. 3B) in both probiotics treated groups (with and without inhibitor) is significantly higher than that in the group with only PI3K inhibitor LY294002. Moreover, the heat map of Fig. 3C shows that the expression of Cdc42 is also increased upon treatment with probiotics. These results demonstrate that probiotics have an up-regulating effect on pathways such as PI3K/Akt-Cdc42-PKC, which probably mobilizes MTOC and Golgi movement to promote cell migration.

In addition to their effects on cell polarization and protrusion, probiotics also manipulate the PI3K signaling pathway to affect adhesion turnover [39, 40]. In a study with neonatal CD-1 mice treated with oral administration of human-derived *Lactobacillus reuteri*, RNA transcriptome analyses of enterocytes showed that *L. reuteri* probiotic intake altered gene expression of several pathways typically involved in cell motility, including integrin-linked kinase (ILK) signaling and integrin signaling, thereby promoting migration [41]. Further, activation of α5β1 integrin was shown to allow the transactivation of beta-catenin gene targets included in an epithelial to mesenchymal (EMT)-like program that induced an increase in glioma cell migration [42]. Notably, hampering cell migration by a specific integrin antagonist provided evidence that the α5β1 integrin/AKT axis was mainly involved in these migration processes, and the activation of key intermediates such as the PKC increased integrin affinity [43]. As mentioned above, probiotics can activate PKC expression via the PI3K/Akt-Cdc42-PKC pathway. In line with this, gene expression analysis showed increased levels of ITG-β1 (Fig. 3B) and ITG-α5 (Fig. 3C) in the presence of probiotics. Taken together, we revealed that probiotics can also promote fibroblast migration by upregulating the expression of ITG genes relevant to the PI3K/Akt-Cdc42-PKC-ITG pathway.

Probiotics BioK influence myofibroblast differentiation of HDFs

The transcriptome results also imply that BioK has an effect on the TGF-β signaling pathway that controls myofibroblast differentiation (Fig. S3). To confirm this, the gene expression of alpha-smooth muscle actin (α-SMA), alpha1 type I collagen (Col-I) and NADPH oxidase 4 (Nox-4) was quantified using qPCR. α-SMA and Col-I are two representative proteins that have been identified as hallmarks of fibrosis and scarring [44], and Nox-4 plays an important role in the transition of fibroblasts to myofibroblasts [45]. A TGF-β treated group was used as a positive control because TGF-β is known to promote myofibroblast differentiation [46]. Expression of fibrosis-related genes varied greatly between all groups. The relative expression levels for α-SMA, Col-I and Nox-4 were higher in the TGF-β group compared to the untreated control, which is consistent with previous reports [44]. When supplementing the TGF-β group with BioK, expression levels decreased from 39.8 to 10.1 fold for Nox-4, from 10.4 to 4.7 fold for α-SMA and from 7.3 to 2.9 fold for Col-I (Fig. 4A-B).

Among the differentiation processes, Smad2 and 3 genes are the most central genes of the TGF-β/Smad signaling pathway to guide the differentiation from fibroblasts to myofibroblasts [47]. Sustained activation of TGF-β/Smad signaling was shown to result in the long-term over-activation of fibroblasts and myofibroblasts, which leads to excessive collagen formation in aberrant scars [46]. Our results demonstrate that the expression of Smad2 and 3 genes is inhibited in the presence of probiotics, and their relative gene expression in the BioK + TGF-β group was reduced to 0.4 and 0.6 folds of that in the TGF-β group (Fig. 4A), respectively, suggesting that probiotics interfere with the expression of the TGF-β /Smad signaling pathway reducing the level of fibrosis.

Immunofluorescence analysis of α-SMA and Col-I was performed after 72 h incubation. TGF-β treated group resulted in a high amount of α-SMA positive cells compared to untreated controls and BioK treated cells, where only few positive cells were observed. Notably, addition of BioK besides TGF-β to HDFs (BioK + TGF-β group) resulted in greatly reduced numbers of α-SMA positive cells compared to the TGF-β positive control (Fig. 4C). As for type I collagen which is synthesized by fibroblasts being a major component of the ECM that forms the scar tissue, the concentration of extracellular collagen Col-I decreased from 9.5 μg/mL to 5.6 μg/mL upon addition of BioK (Fig. 4B). This result is confirmed by the immunostaining assay, where the addition of BioK probiotics led to an apparent inhibitory effect on Col-I production in the BioK + TGF-β group compared to the positive control TGF-β (Fig. 4D). Together, our data illustrate a significant decrease in the expression of biomarkers for myofibroblasts and ECM production in the presence of probiotics, indicating an inhibitory effect on fibrosis.

Acid produced by BioK is a major factor inhibiting the differentiation of HDFs into myofibroblasts

To investigate the underlying factors of BioK that impact myofibroblast differentiation, the role of lactic acid was analyzed because it is produced by BioK in large amounts lowering the local pH dramatically [48]. Acid is known to play a crucial regulatory role in the differentiation of myofibroblasts [49, 50]. Notably, it has been reported that lactate can enhance fibrosis by promoting collagen production in fibroblasts [51]. In this work, we therefore first explored the effect of lactate on HDF differentiation. 10 mM lactate was used for differentiation experiments

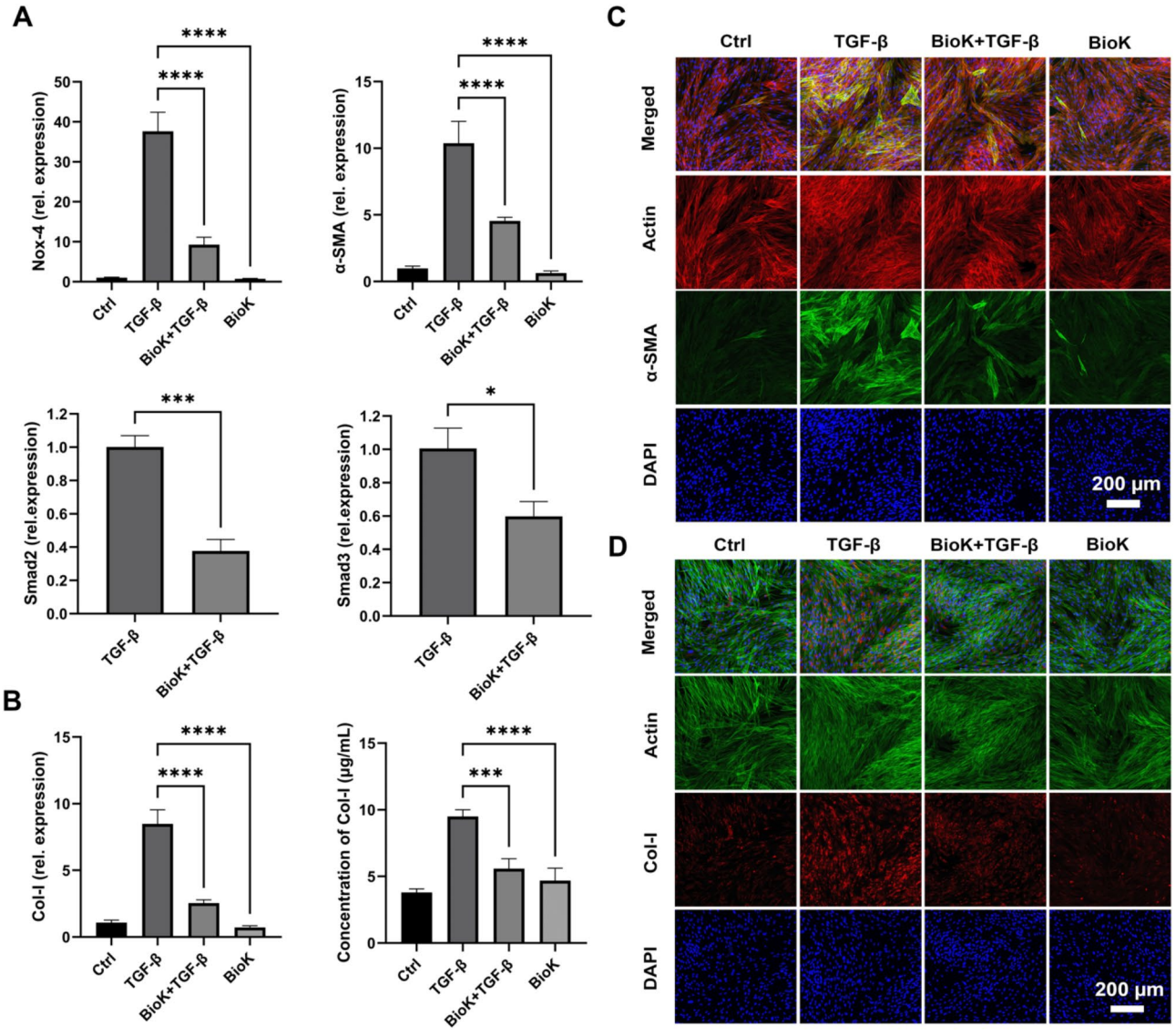

Fig. 4 Influence of probiotics BioK on differentiation of HDF into myofibroblasts. (**A**) Relative gene expression level for Nox-4, α-SMA, Smad2 and Smad3; (**B**) Col-I gene expression (left) and extracellular collagen concentration (right). 'Ctrl' is the blank group without TGF-β or BioK treatment while TGF-β treatment works as the positive control. CLSM images of HDFs cultured for 72 h after staining for (**C**) α-smooth muscle actin (α-SMA, green), actin cytoskeleton (red) and nuclei (blue) and for (**D**) collagen 1 (Col-I, red), actin cytoskeleton (green) and nuclei (blue). Error bars in A&B represent the standard deviation. $n = 3$, *: $P < 0.05$, **: $P < 0.01$, ***: $P < 0.001$, ****: $P < 0.0001$ by ANOVA with a Tukey's post-hoc test

as it was found to be cytocompatible with a cell viability of more than 89% compared to the untreated control (Fig. S7). Quantitative PCR analysis showed that gene expression of α-SMA was increased 2.0-fold in the lactate group, 12.2-fold in the TGF-β group and 16.5-fold in the lactate + TGF-β group, when compared to the untreated control (Fig. 5A), suggesting that lactate has a promoting effect on myofibroblast differentiation. While lactate treatment resulted in few α-SMA positive cells, much higher numbers of positive cells were found in both the TGF-β and lactate + TGF-β group (Fig. 5B). Here, we measured large amounts of lactate in the groups with BioK, accumulating rapidly within the first 48 h and reaching 13.3 mM after 72 h. The concentration of lactate in control groups was maintained at normal levels of cellular metabolism [52, 53], being 0.1 and 1.7 mM for the untreated control and the TGF-β group, respectively (Fig. 5C). Interestingly, while high lactate concentration (produced by BioK) was shown to promote myofibroblast differentiation, probiotics have been reported to inhibit this differentiation. We thus further explored whether the pH reduction can compromise the promoting effect of lactate.

To select a growth medium with lower buffer strength than the standard cell culture medium, i.e. 100% buffered RPMI 1640 medium, and at the same time supporting

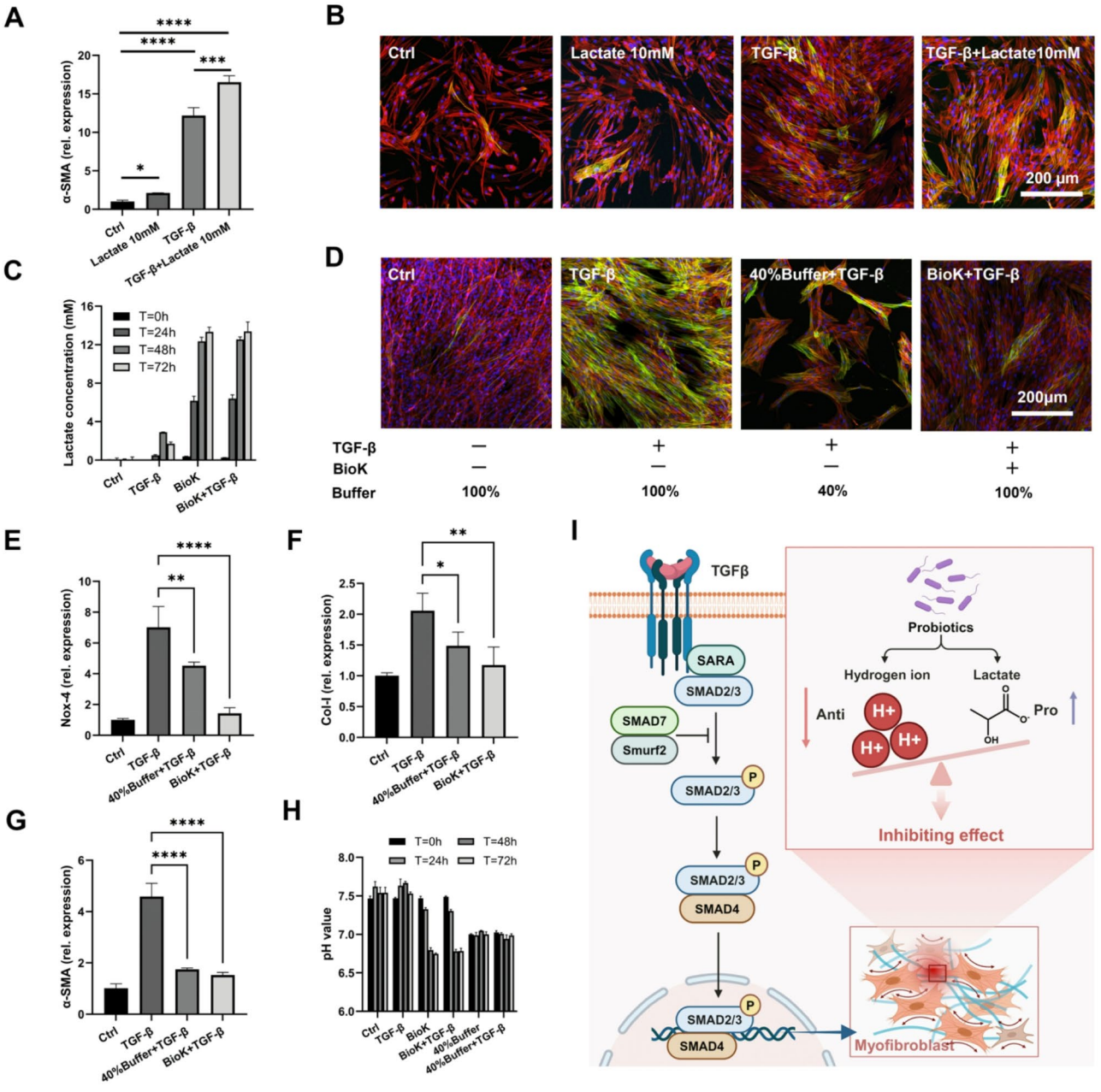

Fig. 5 Inhibition of fibroblast differentiation into myofibroblasts by acid produced by probiotics. (**A**) Relative gene expression level of α-SMA in lactate and TGF-β groups; (**B**) CLSM images of HDFs cultured for 72 h after staining for α-smooth muscle actin (α-SMA, green), actin cytoskeleton (red) and nuclei (blue); (**C**) Lactate production in different groups; (**D**) CLSM images of HDFs cultured for 72 h in different groups after staining for α-smooth muscle actin (α-SMA, green), actin cytoskeleton (red) and nuclei (blue). '-' refers to 'without' while '+' refers to 'with'; Relative expression level of genes associated with myofibroblast differentiation Nox-4 (**E**), Col-I (**F**) and α-SMA (**G**); (**H**) pH changes during cultivation in differentiation media containing probiotics and different concentrations of buffer; (**I**) Schematic of TGF-β-Smad signaling pathway related to fibroblast differentiation and the effects of acid and lactate. "Ctrl" refers to the group with 100% buffer but without any TGF-β, lactate or BioK. Error bars represent the standard deviation. $n = 3$, *: $P < 0.05$, **: $P < 0.01$, ***: $P < 0.001$, ****: $P < 0.0001$ by ANOVA with a Tukey's post-hoc test

HDFs proliferation, media with different buffer strength were screened (Figure S5). Medium containing 40% of the buffer content of normal medium was selected as a positive control (40% buffer + TGF-β) for study of differentiation inhibition. This selection was based on the observation that cells in this medium maintained over 85% relative cell viability in the cytocompatibility assay (Fig. S5C). After 72 h of incubation, cell differentiation and medium pH changes varied greatly between experimental groups. Compared with the untreated control, the positive control TGF-β group significantly promoted the differentiation into myofibroblasts with more α-SMA

positive cells (Fig. 5D), and showed enhanced gene expression of Nox-4, Col-I and α-SMA by 7.0, 2.1 and 4.6 times, respectively (Fig. 5E-G). Noteworthy, the pH of these two groups (untreated and TGF-β) remained stable at pH 7.5 for the entire the culture period (Fig. 5H). However, when we lowered the pH of the medium by decreasing the buffer strength with other conditions and components remaining the same, fibroblast differentiation was significantly inhibited. The starting pH of the medium containing 40% buffer was 7.0 and maintained at 7.0 at the end of incubation (Fig. 5H), but the relative gene expression of Nox-4, Col-I and α-SMA in the 40% buffer group was much lower compared to the TGF-β group, reaching only 4.5, 1.5 and 1.8 fold expression levels, respectively, when compared to the untreated control (Fig. 5E-G). These results suggest that even a slightly reduced pH can hamper myofibroblast differentiation. Similar inhibitory effects were observed for the probiotic-treated group (BioK + TGF-β). α-SMA gene expression was dramatically reduced as observed by the CLSM analysis (Fig. 5D). The qPCR results showed that the expression of Nox-4, Col-I and α-SMA was 1.4, 1.2 and 1.5 fold of the untreated control, respectively. Importantly, all values were much lower than those of the 40% buffer group (Fig. 5E-G). It is important to note that the pH of the co-culture medium changed remarkably in the BioK + TGF-β group, dropping from an initial pH of 7.5 to 7.3 within the first 24 h and remaining at 6.8 up to 72 h (Fig. 5H). When the inhibition of cell differentiation was achieved by lowering the medium pH to pH 7.0 with reduced buffer concentration, this condition also led to drastically lower cell numbers. In contrast, the probiotic treatment also lowered the pH (to pH 6.8), even more than the 40% buffer group, however, this lowered pH did not affect cell numbers and even resulted in the inhibition of myofibroblast differentiation. These results suggest that there are other components produced by probiotics that can compensate the detrimental effect of low pH on cell viability, such as lactate mentioned above. We hypothesize that lactic acid produced by probiotics segregates into hydrogen ions and lactate in an in vitro co-culture environment. On the one hand, the continuous production of hydrogen ions lowered the local pH, an activity that significantly limits myofibroblast differentiation (Fig. 5D-H). On the other hand, ionized lactate acts in the opposite way, promoting fibroblast differentiation (Fig. 5C). The acid ions eventually prevail, allowing for an overall inhibition of differentiation (Fig. 5I).

It is well known that pH plays a role in wound healing [54]. Previous studies have focused on the effect of pH on the activity of matrix metalloproteinases and inhibitors, on the proliferation of fibroblasts and keratinocytes, and on the immunological functions of localized pH changes in the patient's wound [50, 55, 56]. There is no literature detailing which substances from probiotics inhibit fibrosis. A previous report employed *L. plantarum* as probiotic therapy, which significantly reduced both type I collagen mRNA concentration and total collagen protein accumulation in infected wounds, which is consistent with reduced scarring [19]. However, the mechanism by which probiotics inhibit fibrosis was not elucidated. We here demonstrate that the acid produced by probiotics is one of the factors inhibiting cell differentiation from fibroblasts to myofibroblasts. This inhibition is likely achieved by continuously lowering of the pH through the production of acid by probiotics, which is superior to that achieved by altering the buffer content. We cannot rule out the possibility that other factors produced by probiotics might present to facilitate the differentiation inhibition. This warrant further studies to fully understand the role of lactic acid in fibrosis.

Conclusion

Our study aimed to investigate the impact of probiotics on fibroblasts during the remodeling phase of wound-healing and to elucidate the underlying mechanisms. We discovered that probiotics facilitate fibroblast migration, thereby potentially expediting wound healing. Transcriptomic analyses revealed that probiotics BioK upregulate genes such as paxillin, PI3K, PKC, Cdc42, Arp2/3, Rac1, ITG-α5 and ITG-β1, which are associated with the PI3K signaling pathway. We hypothesize that probiotics promote formation of cell membrane protrusions via adjusting genes in the Paxillin-Rac-Arp2/3 pathway, enhance cell polarization by up-regulating genes in the PI3K/Akt-Cdc42-PKC pathway and facilitate cell adhesion turnover via the PI3K/Akt-Cdc42-PKC-ITG pathway, consequently augmenting cell migration. In addition, we found that lactic acid produced by probiotics had an inhibitory effect on the differentiation of fibroblasts to myofibroblasts. This is due to acid produced by probiotics interfering with the TGF/Smad signalling pathway that controls the differentiation process.

However, the mechanisms and signaling pathways that control cell behavior are complex and multi-faceted. Physiological activities such as cell migration are not solely regulated by the PI3K signaling pathway. Other related signaling pathways include for example Ras GTPases, FAK and TorC2 [28, 30, 57]. Moreover, PI3K and these pathways do not work independently of each other but are also intertwined to form a complex network of signaling pathways. Any substance that affects the Ras GTPases, FAK and TorC2 pathways may also affect the PI3K signaling pathway and vice versa. Our results enrich the mechanistic studies of probiotics on enhancing the migration rate of fibroblasts in skin wounds.

In our study, four different probiotic concentrations were initially selected to study the interaction of

probiot-ics and fibroblasts, namely MOI of 0.01, 0.1, 1 and 10, and MOI 10 showed detrimental effect on fibroblasts. Thus, MOI of 0.01, 0.1 and 1 were further investigated in vitro. To translate these concentrations to in vivo experiments, they likely need to be adjusted since in vivo conditions are considerably different from those in vitro. In vivo, fibroblasts reside within the dermis, a highly complex microenvironment composed of multiple cell types and a rich extracellular matrix, which can influence probiotic diffusion, availability, and overall efficacy. As a result, the probiotic concentrations required for in vivo applications may differ from those used in vitro. Furthermore, due to safety and stability considerations, probiotics generally cannot be applied directly to wounds as a simple aqueous solution. Instead, they need to be encapsulated within biomaterial-based delivery systems, which can enhance their stability as well as control the release and overall therapeutic efficacy, as we reported recently [58].

Overall, these findings reveal the promising potential of probiotics in promoting wound healing and combating scar formation. They also provide reference value for clinical treatment and related research. However, it is necessary to further investigate which of the substances produced by probiotics are directly responsible for the promotion of cell migration and inhibition of myofibroblast differentiation. Furthermore, keratinocytes also contribute to scar formation by mediating keratinocyte-fibroblast crosstalk. Specifically, they secrete TGF-β1, which induces the differentiation of fibroblasts into myofibroblasts—cells responsible for collagen deposition and wound contraction. Investigating the cascade of cellular interactions between keratinocyte and HDFs mediated by probiotics could offer significant insights from both a scientific and clinical perspective. In addition, an in vivo study to confirm the capability of probiotics to inhibit scar formation is required.

Abbreviations

ECM	Extracellular matrix
PI3K	Phosphatidylinositol 3-kinase
Akt	Protein kinase B
TGF-β1	Transforming growth factor β1
HDFs	Human dermal fibroblasts
CLSM	Confocal laser scanning microscopy
PCA	Principal component analysis
FPKM	Fragments Per Kilobase per Million mapped fragments
GO	Gene Ontology
KEGG	Kyoto Encyclopedia of Genes and Genomes
Cdc42	Cell division control protein 42 gene
MTOC	Microtubule-organizing center
PKC	Atypical protein kinase C
ILK	Integrin-linked kinase
α-SMA	alpha-Smooth muscle actin
Col-I	Alpha1 type I collagen
Nox-4	NADPH oxidase 4
FCS	Fetal calf serum
RPMI 1640	Roswell Park Memorial Institute
HS	Horse serum
ITG	Integrin
MOI	Multiplicity of infection
FITC	Fluorescein isothiocyanate
DAPI	4′,6-diamidino-2-phenylindole
HPLC	High performance liquid chromatography
RT-qPCR	Reverse transcriptase quantitative polymerase chain reaction

Supplementary Information

The online version contains supplementary material available at https://doi.org/10.1186/s12964-025-02179-y.

Supplementary Material 1

Acknowledgements
We thank members of the Biointerfaces lab for technical support and helpful discussions.

Author contributions
S.Z. contributed to methodology, validation, formal analysis, investigation, visualization, and writing of the original draft and editing. Y.E.-G. and S.T. performed methodology, investigation, and validation. S.S. participated in methodology, investigation, and validation. Z.L. contributed to conceptualization and writing (review and editing). M.R. provided supervision, contributed to methodology, and participated in writing (review and editing). K.M.-W. supervision, managed administration, and contributed to writing (review and editing). Q.R. led the conceptualization, methodology, validation, supervision, project administration, and writing (review and editing).

Funding
This work was supported by grants from the China Scholarship Council (CSC 202006920022) and Schweizerischer Nationalfonds (SNF) (project Nr.: 310030_197617/1).

Data availability
Data available on request.

Declarations

Competing interests
The authors declare no competing interests.

Author details
[1]Empa, Swiss Federal Laboratories for Materials Science and Technology, Biointerfaces Lab, St. Gallen 9014, Switzerland
[2]ETH Zurich, D-BSSE (Department of Biosystems Science and Engineering), Basel 4056, Switzerland

Received: 23 November 2024 / Accepted: 27 March 2025
Published online: 23 April 2025

References

1. Gurtner GC, Werner S, Barrandon Y, Longaker MT. Wound repair and regeneration. Nature. 2008;453(7193):314–21.
2. Peña OA, Martin P. Cellular and molecular mechanisms of skin wound healing. Nat Rev Mol Cell Biol. 2024;25(8):599–616.
3. Ma Y, Liu Z, Miao L, Jiang X, Ruan H, Xuan R, Xu S. Mechanisms underlying pathological scarring by fibroblasts during wound healing. Int Wound J. 2023;20(6):2190–206.
4. Li L, He Y, Zhao M, Jiang J. Collective cell migration: implications for wound healing and cancer invasion. Burns Trauma. 2013;1(1):21–6.
5. Vitorino P, Hammer M, Kim J, Meyer T. A steering model of endothelial sheet migration recapitulates monolayer integrity and directed collective migration. Mol Cell Biol. 2011;31(2):342–50.
6. Ridley AJ, Schwartz MA, Burridge K, Firtel RA, Ginsberg MH, Borisy G, Parsons JT, Horwitz AR. Cell migration: integrating signals from front to back. Science. 2003;302(5651):1704–9.
7. Henderson NC, Rieder F, Wynn TA. Fibrosis: from mechanisms to medicines. Nature. 2020;587(7835):555–66.
8. desJardins-Park HE, Foster DS, Longaker MT. Fibroblasts and wound healing: an update. Regen Med. 2018;13(5):491–5.

9. Cialdai F, Risaliti C, Monici M. Role of fibroblasts in wound healing and tissue remodeling on Earth and in space. Front Bioeng Biotechnol. 2022;10:958381.
10. Olas B. Probiotics, prebiotics and Synbiotics—A promising strategy in prevention and treatment of cardiovascular diseases? Int J Mol Sci. 2020;21(24):9737.
11. Bainbridge P. Wound healing and the role of fibroblasts. J Wound Care. 2013;22(8):407–8.
12. Mohseni AH, Casolaro V, Bermúdez-Humarán LG, Keyvani H, Taghinezhad-S S. Modulation of the PI3K/Akt/mTOR signaling pathway by probiotics as a fruitful target for orchestrating the immune response. Gut Microbes. 2021;13(1):1886844.
13. Tarapatzi G, Filidou E, Kandilogiannakis L, Spathakis M, Gaitanidou M, Arvanitidis K, Drygiannakis I, Valatas V, Kotzampassi K, Manolopoulos VG, et al. The probiotic strains Bifidobacterium lactis, Lactobacillus acidophilus, Lactiplantibacillus plantarum and Saccharomyces boulardii regulate wound healing and chemokine responses in human intestinal subepithelial myofibroblasts. Pharmaceuticals. 2022;15(10):1293.
14. Han N, Jia L, Su Y, Du J, Guo L, Luo Z, Liu Y. Lactobacillus reuteri extracts promoted wound healing via PI3K/AKT/β-catenin/TGFβ1 pathway. Stem Cell Res Ther. 2019;10(1):243.
15. Wei Y, Han Z, Mao X. Injectable living probiotic dressing built by Droplet-Based microfluidics and Photo-Cross-Linking to prevent pathogenic infection and promote wound repair. Adv Healthc Mater. 2024;13(4):2302423.
16. Chen Y, Huang X, Liu A, Fan S, Liu S, Li Z, Yang X, Guo H, Wu M, Liu M, et al. Lactobacillus reuteri vesicles regulate mitochondrial function of macrophages to promote mucosal and cutaneous wound healing. Adv Sci. 2024;11(24):2309725.
17. Sun Y, Liu M, Tang X, Zhou Y, Zhang J, Yang B. Culture-Delivery live probiotics dressing for accelerated infected wound healing. ACS Appl Mater Interfaces. 2023;15(46):53283–96.
18. Dou Z, Li B, Wu L, Qiu T, Wang X, Zhang X, Shen Y, Lu M, Yang Y. Probiotic-Functionalized silk fibroin/sodium alginate scaffolds with Endoplasmic reticulum Stress-Relieving properties for promoted scarless wound healing. ACS Appl Mater Interfaces. 2023;15(5):6297–311.
19. Satish L, Gallo PH, Johnson S, Yates CC, Kathju S. Local probiotic therapy with Lactobacillus plantarum mitigates Scar formation in rabbits after burn injury and infection. Surg Infect. 2017;18(2):119–27.
20. Anders S, Huber W. Differential expression analysis for sequence count data. Genome Biol. 2010;11(10):R106.
21. Love MI, Huber W, Anders S. Moderated Estimation of fold change and dispersion for RNA-seq data with DESeq2. Genome Biol. 2014;15(12):550.
22. Young MD, Wakefield MJ, Smyth GK, Oshlack A. Gene ontology analysis for RNA-seq: accounting for selection bias. Genome Biol. 2010;11(2):R14.
23. Kanehisa M, Goto S. KEGG: Kyoto encyclopedia of genes and genomes. Nucleic Acids Res. 2000;28(1):27–30.
24. Wang Z, Gerstein M, Snyder M. RNA-Seq: a revolutionary tool for transcriptomics. Nat Rev Genet. 2009;10(1):57–63.
25. Hemmings BA, Restuccia DF. PI3K-PKB/Akt pathway. Cold Spring Harb Perspect Biol. 2012;4(9):a011189.
26. Lauffenburger DA, Horwitz AF. Cell migration: A physically integrated molecular process. Cell. 1996;84(3):359–69.
27. Mitchison TJ, Cramer LP. Actin-Based cell motility and cell locomotion. Cell. 1996;84(3):371–9.
28. Brown MC, Turner CE. Paxillin: adapting to change. Physiol Rev. 2004;84(4):1315–39.
29. Vindis C, Teli T, Cerretti DP, Turner CE, Huynh-Do U. EphB1-mediated cell migration requires the phosphorylation of paxillin at Tyr-31/Tyr-118 *. J Biol Chem. 2004;279(27):27965–70.
30. Deakin NO, Turner CE. Paxillin comes of age. J Cell Sci. 2008;121(15):2435–44.
31. Dise RS, Frey MR, Whitehead RH, Polk DB. Epidermal growth factor stimulates Rac activation through Src and phosphatidylinositol 3-kinase to promote colonic epithelial cell migration. Am J Physiology-Gastrointestinal Liver Physiol. 2008;294(1):G276–85.
32. Itoh RE, Kurokawa K, Ohba Y, Yoshizaki H, Mochizuki N, Matsuda M. Activation of Rac and Cdc42 video imaged by fluorescent resonance energy Transfer-Based Single-Molecule probes in the membrane of living cells. Mol Cell Biol. 2002;22(18):6582–91.
33. Tybulewicz VLJ, Ardouin L, Prisco A, Reynolds LF. Vav1: a key signal transducer downstream of the TCR. Immunol Rev. 2003;192(1):42–52.
34. Devreotes P, Horwitz AR. Signaling networks that regulate cell migration. Cold Spring Harb Perspect Biol. 2015;7(8):a005959.
35. Welch HCE, Coadwell WJ, Stephens LR, Hawkins PT. Phosphoinositide 3-kinase-dependent activation of Rac. FEBS Lett. 2003;546(1):93–7.
36. Etienne-Manneville S, Hall A. Rho GTPases in cell biology. Nature. 2002;420(6916):629–35.
37. Rodriguez OC, Schaefer AW, Mandato CA, Forscher P, Bement WM, Waterman-Storer CM. Conserved microtubule–actin interactions in cell movement and morphogenesis. Nat Cell Biol. 2003;5(7):599–609.
38. Etienne-Manneville S, Hall A. Cell Polarity: Par6, aPKC and cytoskeletal crosstalk. Curr Opin Cell Biol. 2003;15(1):67–72.
39. Emsley J, Knight CG, Farndale RW, Barnes MJ, Liddington RC. Structural basis of collagen recognition by integrin A2β1. Cell. 2000;101(1):47–56.
40. Geiger B, Bershadsky A, Pankov R, Yamada KM. Transmembrane crosstalk between the extracellular matrix and the cytoskeleton. Nat Rev Mol Cell Biol. 2001;2(11):793–805.
41. Preidis GA, Saulnier DM, Blutt SE, Mistretta T-A, Riehle KP, Major AM, Venable SF, Finegold MJ, Petrosino JF, Conner ME, et al. Probiotics stimulate enterocyte migration and microbial diversity in the neonatal mouse intestine. FASEB J. 2012;26(5):1960–9.
42. Renner G, Noulet F, Mercier M-C, Choulier L, Etienne-Selloum N, Gies J-P, Lehmann M, Lelong-Rebel I, Martin S, Dontenwill M. Expression/activation of A5β1 integrin is linked to the β-catenin signaling pathway to drive migration in glioma cells. Oncotarget. 2016;7(38):62194–207.
43. Kim M, Carman CV, Springer TA. Bidirectional transmembrane signaling by cytoplasmic domain separation in integrins. Science. 2003;301(5640):1720–5.
44. Guex AG, Poxson DJ, Simon DT, Berggren M, Fortunato G, Rossi RM, Maniura-Weber K, Rottmar M. Controlling pH by electronic ion pumps to fight fibrosis. Appl Mater Today. 2021;22:100936.
45. Siedlar AM, Seredenina T, Faivre A, Cambet Y, Stasia M-J, André-Lévigne D, Bochaton-Piallat M-L, Pittet-Cuénod B, de Seigneux S, Krause K-H, et al. NADPH oxidase 4 is dispensable for skin myofibroblast differentiation and wound healing. Redox Biol. 2023;60:102609.
46. Zhang T, Wang X-F, Wang Z-C, Lou D, Fang Q-Q, Hu Y-Y, Zhao W-Y, Zhang L-Y, Wu L-H. Tan W-Q: current potential therapeutic strategies targeting the TGF-β/Smad signaling pathway to attenuate keloid and hypertrophic Scar formation. Biomed Pharmacother. 2020;129:110287.
47. Khalil H, Kanisicak O, Prasad V, Correll RN, Fu X, Schips T, Vagnozzi RJ, Liu R, Huynh T, Lee S-J, et al. Fibroblast-specific TGF-β–Smad2/3 signaling underlies cardiac fibrosis. J Clin Investig. 2017;127(10):3770–83.
48. Li Z, Zhang S, Zuber F, Altenried S, Jaklenec A, Langer R, et al. Topical application of lactobacilli successfully eradicates Pseudomonas aeruginosa biofilms and promotes wound healing in chronic wounds. Microbes Infect. 2023;25(8):105176.
49. Kruse CR, Singh M, Targosinski S, Sinha I, Sørensen JA, Eriksson E, Nuutila K. The effect of pH on cell viability, cell migration, cell proliferation, wound closure, and wound reepithelialization: in vitro and in vivo study. Wound Repair Regeneration. 2017;25(2):260–9.
50. Sharpe JR, Harris KL, Jubin K, Bainbridge NJ, Jordan NR. The effect of pH in modulating skin cell behaviour. Br J Dermatol. 2009;161(3):671–3.
51. Wu H, Liang W, Han M, Zhen Y, Chen L, Li H, An Y. Mechanisms regulating wound healing: functional changes in biology mediated by lactate and histone lactylation. J Cell Physiol. 2023;238(10):2243–52.
52. Li X, Yang Y, Zhang B, Lin X, Fu X, An Y, Zou Y, Wang J-X, Wang Z, Yu T. Lactate metabolism in human health and disease. Signal Transduct Target Therapy. 2022;7(1):305.
53. Brooks GA. Lactate as a fulcrum of metabolism. Redox Biol. 2020;35:101454.
54. Percival SL, McCarty S, Hunt JA, Woods EJ. The effects of pH on wound healing, biofilms, and antimicrobial efficacy. Wound Repair Regeneration. 2014;22(2):174–86.
55. Lardner A. The effects of extracellular pH on immune function. J Leukoc Biol. 2001;69(4):522–30.
56. HEMING TA, DAVÉ SK, TUAZON DM, CHOPRA AK, PETERSON JW, BIDANI A. Effects of extracellular pH on tumour necrosis factor-α production by resident alveolar macrophages. Clin Sci. 2001;101(3):267–74.
57. Cai H, Das S, Kamimura Y, Long Y, Parent CA, Devreotes PN. Ras-mediated activation of the TORC2–PKB pathway is critical for chemotaxis. J Cell Biol. 2010;190(2):233–45.
58. Tao S, Zhang S, Wei K, Maniura-Weber K, Li Z, Ren Q. An injectable living hydrogel with embedded probiotics as a novel strategy for combating multifaceted pathogen wound infections. Adv Healthc Mater. 2024;13(27):2400921.

Publisher's note